

SA-IQA: Redefining Image Quality Assessment for Spatial Aesthetics with Multi-Dimensional Rewards

Yuan Gao, Jin Song
Alibaba Group

ayuan.gy@taobao.com, songjin.song@alibaba-inc.com

Abstract

In recent years, Image Quality Assessment (IQA) for AI-generated images (AIGI) has advanced rapidly; however, existing methods primarily target portraits and artistic images, lacking a systematic evaluation of interior scenes. We introduce *Spatial Aesthetics*, a paradigm that assesses the aesthetic quality of interior images along four dimensions: layout, harmony, lighting, and distortion. We construct **SA-BENCH**, the first benchmark for spatial aesthetics, comprising 18,000 images and 50,000 precise annotations. Employing **SA-BENCH**, we systematically evaluate current IQA methodologies and develop **SA-IQA**, through MLLM fine-tuning and a multidimensional fusion approach, as a comprehensive reward framework for assessing spatial aesthetics. We apply **SA-IQA** to two downstream tasks: (1) serving as a reward signal integrated with GRPO reinforcement learning to optimize the AIGC generation pipeline, and (2) Best-of-N selection to filter high-quality images and improve generation quality. Experiments indicate that **SA-IQA** significantly outperforms existing methods on **SA-BENCH**, setting a new standard for spatial aesthetics evaluation. Code and dataset will be open-sourced to advance research and applications in this domain.

1. Introduction

The growth of Generative Artificial Intelligence (AIGC) has made Image Quality Assessment (IQA) increasingly important. IQA has two main roles: one is to filter low-quality generated content, and the second is to be used as a human preference alignment signal for post-training generative models [30]. Therefore, the evaluation content of IQA has also evolved from early traditional image quality (such as blur or noise) [34] to the current stage’s complex human preferences, such as image aesthetics [7], human anatomy [16], text-image alignment [38], and the latest instruction following in image editing [6].

Along with the change in IQA’s research focus, the re-

search methods have also evolved from being based on early pre-trained models like CLIP [23] to leveraging Multimodal Large Language Models (MLLMs), like Q-Align [27], which perform finer-grained, human-aligned evaluations by utilizing the capabilities of large pre-trained models.

AI is being rapidly and widely adopted in applications like interior design and furniture e-commerce. However, existing IQA methods are often trained on general-purpose datasets [10, 14] that cover mass aesthetic preferences. While specialized benchmarks for domains like human figures [16] or artistic style [36] exist, there is currently no dataset or corresponding IQA method dedicated to interior design spatial aesthetics. This evaluation of “Spatial Aesthetics” is extremely complex, demanding the concurrent evaluation of multiple factors: the layout of objects within the space, the harmony of style and color, the consistency and coordination of lighting, and the presence of AI-induced environmental distortions or artifacts.

To comprehensively address the application of IQA in spatial aesthetics, evaluate and improve the quality of AI-generated interior images, we first construct a high-quality dataset with multi-dimensional human annotations and train a IQA model based on this dataset. Specifically, our contributions are:

- **SA-BENCH:** We define the Spatial Aesthetics paradigm along four dimensions—layout, harmony, lighting, and distortion—and construct the first benchmark comprising 18,000 interior images with 50,000 precise human annotations. The visualization of a portion of the dataset is shown in Figure 1.
- **SA-IQA:** We introduce a Spatial Aesthetics IQA model that outputs calibrated, multi-dimensional rewards (layout, harmony, lighting, distortion). Built via MLLM fine-tuning with expert-aware instructions and a multidimensional fusion optimization, **SA-IQA** attains state-of-the-art PLCC/SROCC on **SA-BENCH**.
- **Downstream Applications:** We fully validate the effectiveness of our **SA-IQA** model in two representative downstream tasks: first, we integrate **SA-IQA** as a reward

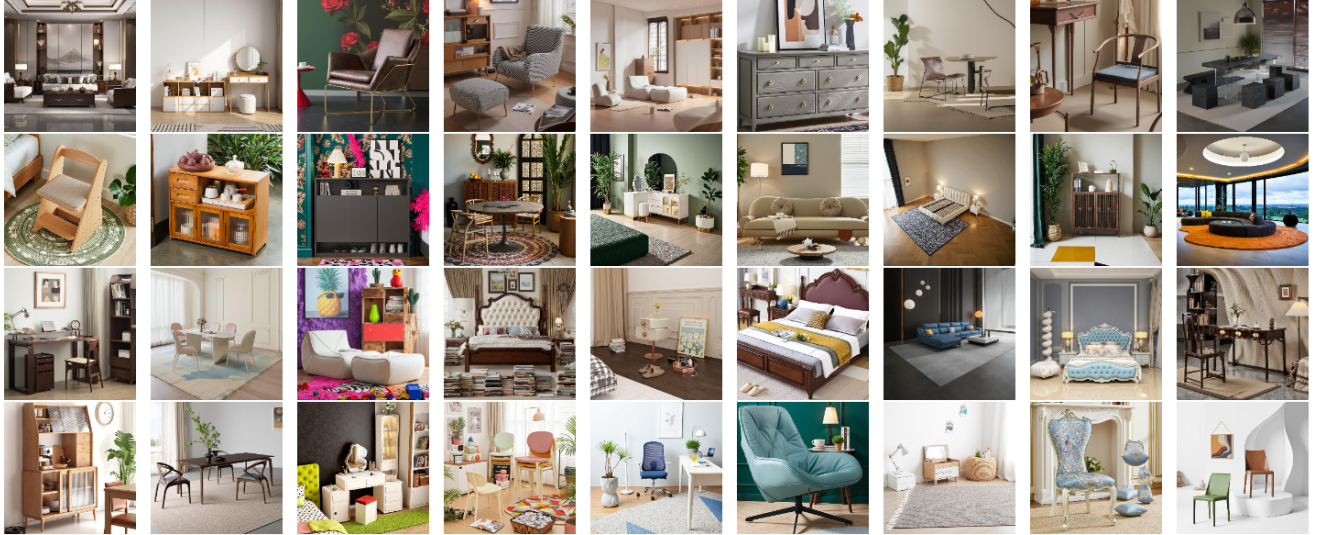


Figure 1. **Visualizing the SA-BENCH dataset.** From top to bottom, each row corresponds to the results of different models in the dataset: the first row uses SD1.5-Inpaint [20], the second row is SDXL-BrushNet [8], the third row is FLUX-Inpaint [11], and the fourth row is FLUX EasyControl [41].

signal, in conjunction with GRPO, to optimize a prompt expansion module for image generation task, and second, in Best-of-N selection to filter low-quality images, significantly improving generation quality.

2. Related Work

2.1. Text-to-Image

The field of text-to-image (T2I) generation has grown rapidly. Open-source models like Stable Diffusion (SD) [20], SDXL [18], and SD3 [4] continue to improve image realism. Commercial models such as Midjourney and Seedream4.0 [21] can already generate highly realistic images. The training pipeline for these models often includes pre-training, fine-tuning, and reinforcement learning (RL) stages to align with human preferences, which requires collecting large-scale preference data.

Although some open-source aesthetic preference datasets exist, such as ImageReward [31] and HPSV2 [28], this data often reflects general preferences. This can lead to a lack of precision when working in specific domains, like interior design. To fix this, some methods collect domain-specific preference data. For instance, flux-krea [12] collected its data in a “very opinionated manner” to match a specific aesthetic taste and a “clear art direction.” Similarly, other methods have used preference data focused on anatomical distortions to improve how models generate human anatomy [16].

2.2. Image Quality Assessment

Early IQA benchmarks for AIGI started to define the key evaluation factors. For example, AGIQA-3K [13] and AIG-CIQA2023 [24] were among the first to use multidimensional assessments. They moved beyond a single quality score to measure factors like perceptual quality, authenticity, and text-to-image correspondence. This approach was later scaled up by AIGIQA-20K [14].

However, these benchmarks remain general-purpose and have limits when applied to specific, structurally-complex domains. A key development in the field is therefore the creation of domain-specific IQA. A clear example is AGHI-QA [16], which argues that general-purpose models “fail to deliver fine-grained perceptual evaluations for structurally complex subjects like humans.” To solve this, AGHI-QA provides detailed structural annotations for *distorted body parts* (e.g., face, hands, body).

Building directly on this idea, our work identifies **interior scenes** as another critical, yet unaddressed, structurally complex domain. We propose **Spatial Aesthetics** as a new paradigm to break down quality assessment into domain-slowng, structural, and aesthetic attributes: *layout, harmony, lighting, and distortion*.

Methodologically, the field has quickly moved towards using Multimodal Large Language Models (MLLMs) as assessors. This shift moves beyond “black box” scores to provide judgments that are explainable and aligned with human reasoning. Q-ALIGN [27] was an early example of this, training MLLMs to use “discrete text-defined levels” (e.g., “excellent”, “good”, “bad”) rather than predicting a continuous score.

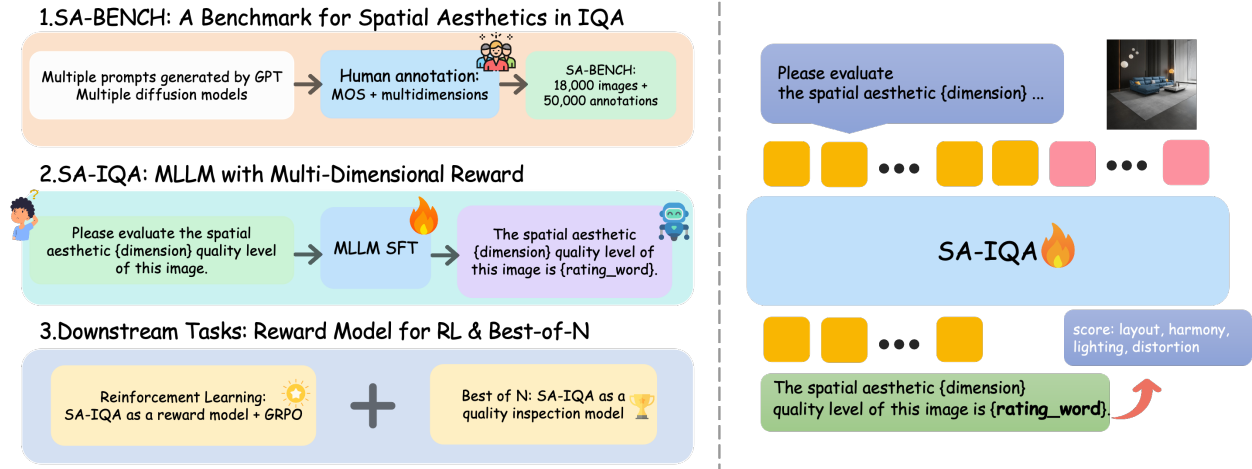


Figure 2. **Overview of the SA-IQA Framework.** The left panel depicts our three-stage workflow: establishing Spatial Aesthetics dimensions and constructing SA-BENCH, developing the SA-IQA reward model via MLLM fine-tuning, and deploying it for GRPO-based prompt optimization and Best-of-N selection. The right panel details the SA-IQA model’s principle, showing how it processes an image and a dimension-conditioned query to predict multi-dimensional MOS scores, which are then calibrated and fused into a single spatial aesthetic score.

This approach was extended by Q-Insight [15], which used reinforcement learning (specifically GRPO) to get robust reasoning from limited reward signals. At the same time, GROUNDING-IQA [3] pushed IQA beyond global analysis to fine-grained spatial assessment. It “integrates multimodal referring and grounding with IQA” to provide detailed quality descriptions along with “precise locations (i.e., bounding boxes)” for low-quality regions.

Our proposed SA-IQA combines these state-of-the-art ideas: it is an explainable, MLLM-based framework, designed for our new domain-specific benchmark (SA-BENCH), to perform multidimensional and spatially-aware assessment.

3. Method

We propose **SA-IQA**, a novel framework designed to address the unique challenges of interior spatial aesthetics evaluation. As shown in Figure 2, it comprises three stages: (1) the creation of “SA-BENCH”, a specialized multi-dimensional benchmark through rigorous human annotation; (2) the development of the “SA-IQA” model via MLLM Supervised Fine-Tuning (SFT) and a multi-dimensional fusion module; and (3) the application of SA-IQA in “Downstream Tasks” (Reinforcement Learning optimization and Best-of-N selection) to enhance the quality of AIGC outputs.

3.1. SA-BENCH

3.1.1. Benchmark overview

We introduce SA-BENCH, a benchmark tailored to spatial aesthetics of interior AIGI with four dimensions—layout,

harmony, lighting, and distortion—and high-quality MOS annotations. SA-BENCH comprises 17753 images and 50476 precise annotations, establishing the first large-scale, multi-dimensional interior benchmark for spatial-aesthetics IQA. Table 1 highlights SA-BENCH’s coverage compared with representative IQA/aesthetics datasets.

3.1.2. Data Construction

We begin with a large pool of real-world interior photographs as raw data. To reduce redundancy, we first extract image features using DreamSim [5] and apply K-means clustering to remove highly similar samples. For the remaining images, we extract the main object mask using BiRefNet [45].

Next, we generate a base prompt from the real image using Qwen2.5-VL [1]. This prompt is then intentionally corrupted using ChatGPT. The purpose of this corruption is to create inputs that will cause the generative models to produce low-score (low-quality) images. This process yields nine prompts of varying quality for each object.

Finally, we use these nine prompts and their corresponding object masks to generate images with four different inpainting models: SD1.5-Inpaint, SDXL-BrushNet [8], FLUX-Inpaint, and FLUX EasyControl [41]. Among these, the SD1.5-Inpaint and FLUX-Inpaint models were obtained by fine-tuning their respective base text-to-image models (SD1.5 [20] and FLUX [11]) by concatenating the mask and the masked-image to the input layer. For each real image, this entire pipeline yields $9 \times 4 = 36$ AI-generated images covering a broad range of qualities and styles.

Table 1. Comparison of different AIGC Quality Datasets.

| Database | Annotation Type | Dimensions | Images | Annotations | Generation Models |
|------------------|-----------------|-----------------------|-----------|-------------|-------------------|
| DiffosonDB[26] | No | No | 1,819,808 | 0 | 1 |
| AGIQA-1K [42] | MOS | Perception | 1,080 | 23,760 | 2 |
| Pick-A-Pic [10] | Preference | Overall | 500,000 | 500,000 | 3 |
| HPS[29] | Preference | Overall | 98,807 | 98,807 | 1 |
| ImageReward [32] | Ranking | Perception; Alignment | 136,892 | 410,676 | 7 |
| AGIQA-3K [13] | MOS | Perception; Alignment | 2,982 | 125,244 | 8 |
| SA-BENCH | MOS | Spatial Aesthetics | 17,753 | 50,476 | 4 |



Figure 3. **Sample annotation examples from the SA-Bench.** For each quality dimension (Layout, Harmony, Lighting, and Distortion), five representative examples are presented, spanning quality levels from *bad* (1) to *excellent* (5). These examples serve as crucial visual guidelines for human annotators, ensuring consistent and high-quality scoring throughout our benchmark.

3.1.3. Annotation protocol

Each image is independently rated on a 1–5 score by 1–5 professionally trained interior designers; most images receive five independent ratings. Figure 3 illustrates representative examples for different quality levels across the four dimensions, while Figure 4 shows the resulting score distributions. The four dimensions are defined as follows:

- **Layout:** Spatial arrangement of key elements, their relative positions, and object counts. Typical problems include excessive emptiness, clutter, and poor placement.
- **Harmony:** Stylistic coherence, color compatibility, and overall visual consistency. Typical problems include color clashes, mismatched design styles, and generally unattractive appearance.
- **Lighting:** Quality of illumination, shadow behavior, and realism of light sources. Typical problems include unnatural lighting, incorrect or inconsistent shadows, and implausible light sources.
- **Distortion:** Geometric or semantic deformation of fur-

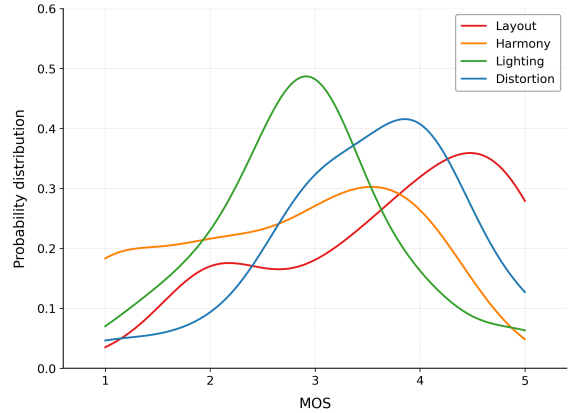


Figure 4. **MOS Distribution on SA-Bench.** The plot shows the probability distribution of Mean Opinion Scores (MOS) for each of the four dimensions (Layout, Harmony, Lighting, and Distortion), illustrating the range and concentration of scores from 1 (bad) to 5 (excellent).

nishings/fixtures and the realism of materials. Typical problems include warped or distorted backgrounds, shape deformation, and unconvincing materials.

3.1.4. Cleaning and reliability

Acceptance auditing. We audit 10% of annotations; batches falling below 85% accuracy are returned for re-annotation.

Score aggregation. We compute the Mean Opinion Score (MOS) to aggregate N_i ratings (s_{ij}) and reduce annotator bias:

$$\text{MOS}_{i,d} = \frac{1}{N_i} \sum_{j=1}^{N_i} s_{ij} \quad (1)$$

Rater reliability. We compute the SRCC between annotator scores and the MOS. Annotators with $\text{SRCC} < 0.6$ are flagged for review.

Outlier mitigation. We standardize ratings (z-score) to identify outliers. Ratings with an absolute z-score > 2 are replaced by the mean, and the MOS is recomputed.

Finally, SA-BENCH contains 17,753 images and 50,476 annotations, providing the first large-scale benchmark for

Table 2. Statistics of the SA Benchmark Dataset.

| Dimension | Annotations | Train | Test | Total |
|--------------|---------------|--------|-------|---------------|
| Layout | 23,615 | 4,444 | 1,098 | 5,542 |
| Harmony | 19,615 | 5,392 | 1,348 | 6,740 |
| Lighting | 4,546 | 2,596 | 649 | 3,245 |
| Distortion | 2,700 | 1,780 | 446 | 2,226 |
| Total | 50,476 | 14,212 | 3,541 | 17,753 |

indoor spatial aesthetic IQA (Table 2).

3.2. SA-IQA

3.2.1. IQA model

Model Architecture and Fine-Tuning Our SA-IQA model is built upon the Ovis2.5 [17] MLLM backbone, chosen for its strong high-resolution and spatial sensitivity. We perform supervised fine-tuning (SFT) on our SA-BENCH train dataset to assess four aesthetic dimensions: layout, harmony, lighting, and distortion. As shown in Figure 2, the model processes an image and a dimension-specific text query (Type 4, Table 4) that explicitly defines the target dimension and its evaluation criteria. We attach a dimension tag (e.g., <Layout>) within the prompt. The model outputs a structured response with a specific rating word, such as *excellent*, *good*, *fair*, *poor*, or *bad*.

Score Computation To convert this categorical text rating into a continuous MOS score, we employ a probabilistic method inspired by *Q-Align*[27]. This process involves extracting the top-5 probabilities for the five predefined rating words (e.g., *excellent* to *bad*) from the MLLM’s final quality word token. After softmax normalization, we compute the expected value over a 1-5 scale (e.g., *excellent*→5, *bad*→1) to derive the final score within the range [1, 5].

3.2.2. Multidimensional Score Fusion

Downstream applications, such as reinforcement learning, often require a single composite quality score rather than multiple dimensional assessments. Therefore, we fuse the four dimension-specific scores into a single composite quality score by learning optimal weights using a Bradley–Terry (BT) [2] rank-likelihood objective. We construct a rank dataset of 750 image pairs, where annotators provide pairwise preferences (“Image A better,” “Image B better,” or “Tie”) for overall spatial aesthetics. For each pair of images (I_A, I_B), we first compute their respective four-dimensional score vectors, \mathbf{x}_A and \mathbf{x}_B , using our SA-IQA model.

We then learn a set of optimal fusion weights \mathbf{w} to compute a final scalar score $S = \mathbf{x}^\top \mathbf{w}$. To find these weights, we fit a Bradley–Terry (BT) model. This model defines

the probability of I_A being preferred over I_B as a function of their weighted score difference: $P(A > B) = \sigma(S_A - S_B) = \sigma((\mathbf{x}_A - \mathbf{x}_B)^\top \mathbf{w})$.

We optimize \mathbf{w} by minimizing the negative log-likelihood (BT-loss) between the model’s predicted probabilities and the human-annotated preference labels:

$$\mathcal{L}(\mathbf{w}) = -\mathbb{E} \left[y \log \sigma(\Delta \mathbf{x}^\top \mathbf{w}) + (1-y) \log (1 - \sigma(\Delta \mathbf{x}^\top \mathbf{w})) \right] \quad (2)$$

where $\Delta \mathbf{x} = \mathbf{x}_A - \mathbf{x}_B$ represents the difference between the multidimensional score vectors of the two images in a pair. $y \in \{0, 1\}$ is the ground-truth preference label (e.g., $y = 1$ if I_A is preferred over I_B , $y = 0$ otherwise), derived from the human annotations. $\sigma(\cdot)$ is the sigmoid function. Minimizing this loss yields the optimal fusion weights \mathbf{w}^* .

The final fused score is then computed as a weighted sum of the dimension scores:

$$\text{Score} = \mathbf{x}^\top \mathbf{w}^* = \sum_{i=1}^n x_i w_i^* \quad (3)$$

where x_i are the individual dimension scores and w_i^* are the learned optimal weights.

4. Experiments

4.1. Experimental Setup

Training details: We fine-tune all MLLM via supervised fine-tuning (SFT). Optimization employs AdamW with a weight decay of 0.1 and a warmup ratio of 0.03. The learning rate is set to 2×10^{-5} . Training is conducted on 4 NVIDIA H20 GPUs (96 GB each) using a per-GPU batch size of 2 and gradient accumulation of 32 steps, resulting in an effective global batch size of 256. Only the LLM component of the MLLM is fine-tuned, while the ViT and Aligner components remain frozen. Training proceeds for 3 epochs, and results are reported from the final checkpoint.

Datasets and metrics: SA-BENCH serves as both the training and evaluation benchmark, utilizing a 4:1 train/test split with matched data distributions. We report results for the four individual dimensions—layout, harmony, lighting, and distortion—as well as an “Overall” score derived from the pooled test set. The primary evaluation metrics are the Pearson Linear Correlation Coefficient (PLCC) and Spearman Rank-Order Correlation Coefficient (SRCC) between our model’s predicted scores and human Mean Opinion Scores (MOS).

4.2. IQA Comparisons

We systematically evaluate various IQA approaches on SA-BENCH, categorized into: (i) Traditional NR-IQA methods, (ii) Deep Learning-based NR-IQA models, (iii) Commercial MLLMs, and (iv) our SA-IQA framework utilizing Supervised Fine-Tuning (SFT-based MLLMs). Table 3

Table 3. PLCC/SRCC performance comparison on SA-BENCH. Best results are **bolded**, and second-best results are underlined.

| Method Category | Layout | Harmony | Lighting | Distortion | Overall |
|-----------------------------------|----------------------|----------------------|------------------------|----------------------|----------------------|
| Traditional NR-IQA | | | | | |
| MUSIQ[9] | 0.121 / 0.138 | 0.007 / -0.017 | 0.133 / 0.228 | 0.019 / -0.001 | 0.057 / 0.084 |
| DBCNN[40] | 0.162 / 0.173 | -0.006 / -0.007 | 0.198 / 0.197 | 0.105 / 0.096 | 0.082 / 0.1 |
| CLIP-IQA[23] | 0.197 / 0.230 | <u>0.097 / 0.101</u> | 0.062 / 0.084 | <u>0.113 / 0.128</u> | 0.118 / 0.135 |
| MANIQA[33] | <u>0.194 / 0.210</u> | 0.096 / 0.105 | 0.125 / 0.147 | 0.071 / 0.073 | <u>0.118 / 0.139</u> |
| HyperIQA[22] | 0.179 / 0.217 | 0.135 / 0.136 | <u>0.161 / 0.181</u> | 0.163 / 0.131 | 0.144 / 0.165 |
| Deep Learning-based NR-IQA | | | | | |
| Q-Insight[15] | 0.053 / 0.060 | 0.080 / 0.093 | 0.286 / 0.286 | 0.067 / 0.032 | 0.083 / 0.089 |
| Compare2Score[46] | 0.160 / 0.162 | 0.074 / 0.075 | 0.274 / 0.288 | 0.028 / 0.011 | 0.088 / 0.115 |
| DeQA-Score[37] | <u>0.201 / 0.174</u> | 0.139 / 0.105 | 0.305 / 0.351 | 0.025 / 0.006 | 0.111 / 0.141 |
| Q-SiT[44] | <u>0.141 / 0.190</u> | 0.098 / 0.077 | 0.207 / 0.219 | 0.184 / 0.131 | 0.115 / 0.140 |
| Q-Align-quality[27] | 0.057 / 0.101 | <u>0.183 / 0.187</u> | <u>0.299 / 0.294</u> | 0.088 / 0.074 | 0.110 / 0.128 |
| Q-Align-aesthetics[27] | 0.075 / 0.082 | 0.318 / 0.320 | 0.116 / 0.120 | 0.001 / 0.026 | <u>0.133 / 0.142</u> |
| Q-Eval-Score[43] | 0.265 / 0.266 | 0.149 / 0.142 | 0.036 / 0.042 | <u>0.144 / 0.153</u> | 0.162 / 0.168 |
| Commercial MLLMs | | | | | |
| gpt-4o | 0.017 / -0.009 | 0.537 / 0.542 | 0.064 / 0.038 | <u>0.233 / 0.149</u> | 0.312 / 0.298 |
| gpt-5 | <u>0.185 / 0.147</u> | 0.483 / 0.490 | -0.031 / -0.054 | 0.204 / 0.177 | 0.318 / 0.308 |
| claude35_sonnet | -0.001 / -0.032 | <u>0.542 / 0.552</u> | -0.179 / -0.197 | 0.058 / -0.006 | 0.326 / 0.304 |
| qwen-vl-max | 0.088 / 0.067 | 0.526 / 0.528 | -0.037 / -0.058 | 0.091 / 0.078 | <u>0.362 / 0.359</u> |
| gemini-2.5-pro | 0.246 / 0.181 | 0.594 / 0.603 | <u>-0.023 / -0.043</u> | 0.252 / 0.225 | 0.414 / 0.393 |
| MLLMs (SFT-based) | | | | | |
| Ovis2-5-2B[17] | 0.812 / 0.807 | 0.890 / 0.888 | 0.692 / 0.681 | 0.556 / 0.520 | 0.848 / 0.844 |
| mPLUG-Owl3-7B[35] | 0.784 / 0.773 | 0.831 / 0.822 | 0.662 / 0.675 | 0.456 / 0.421 | 0.810 / 0.810 |
| GLM-4-1V-9B[39] | <u>0.831 / 0.821</u> | 0.848 / 0.834 | 0.690 / 0.690 | 0.532 / 0.503 | 0.836 / 0.842 |
| InternVL3-5-8B[25] | 0.774 / 0.769 | 0.885 / 0.882 | 0.702 / 0.693 | 0.539 / 0.462 | 0.837 / 0.829 |
| Qwen3-VL-2B[19] | 0.808 / 0.802 | <u>0.886 / 0.884</u> | 0.684 / 0.687 | 0.481 / 0.439 | 0.841 / 0.836 |
| Qwen3-VL-4B[19] | 0.821 / 0.807 | 0.892 / 0.891 | <u>0.712 / 0.701</u> | <u>0.558 / 0.488</u> | <u>0.853 / 0.849</u> |
| Qwen3-VL-8B[19] | 0.814 / 0.804 | 0.892 / 0.889 | 0.696 / 0.705 | 0.529 / 0.506 | 0.849 / 0.846 |
| SA-IQA(Ours) | 0.831 / 0.822 | 0.896 / 0.895 | 0.724 / 0.694 | 0.657 / 0.596 | 0.864 / 0.860 |

Table 4. PLCC/SRCC performance on SA-BENCH for different prompt types. Best results are **bolded**, and second-best are underlined.

| Prompt Type | Layout | Harmony | Lighting | Distortion | Overall | Description Style |
|-------------|--------------------|--------------------|--------------------|--------------------|----------------------|-------------------|
| Type 1 | 0.829/0.820 | 0.894/0.891 | 0.717/0.697 | <u>0.575/0.552</u> | 0.857/0.855 | Concise |
| Type 2 | 0.825/0.816 | 0.895/0.893 | 0.729/0.711 | 0.572/0.564 | 0.858/0.854 | Concise+ |
| Type 3 | <u>0.830/0.823</u> | 0.898/0.896 | 0.717/0.702 | 0.567/0.555 | <u>0.859/0.856</u> | Detailed |
| Type 4 | 0.831/0.822 | <u>0.896/0.895</u> | <u>0.724/0.694</u> | 0.657/0.596 | 0.864 / 0.860 | Expert-Aware |

presents the PLCC/SRCC correlations with human MOS. Within each category block, the best result is **bolded** and the second best is underlined.

Traditional NR-IQA: These methods exhibit limited performance across all four dimensions of interior spatial aes-

thetics, with correlations typically below 0.20. While CLIP-IQA shows the strongest layout correlation (0.197/0.230) and HyperIQA leads in harmony (0.135/0.136), distortion (0.163/0.131), and overall (0.144/0.165), the significant performance gap to other categories indicates poor gener-

Table 5. PLCC/SRCC performance on SA-BENCH for different MLLM sizes. Best results are **bolded**, and second-best are underlined.

| Method Category | Layout | Harmony | Lighting | Distortion | Overall |
|-----------------|----------------------|----------------------|----------------------|----------------------|----------------------|
| Qwen3-VL-2B | 0.808 / 0.802 | <u>0.886 / 0.884</u> | 0.684 / 0.687 | 0.481 / 0.439 | 0.841 / 0.836 |
| Qwen3-VL-4B | 0.821 / 0.807 | <u>0.892 / 0.891</u> | <u>0.712 / 0.701</u> | <u>0.558 / 0.488</u> | <u>0.853 / 0.849</u> |
| Qwen3-VL-8B | 0.814 / 0.804 | 0.892 / 0.889 | <u>0.696 / 0.705</u> | <u>0.529 / 0.506</u> | 0.849 / 0.846 |
| Ovis2-5-2B | 0.812 / 0.807 | 0.890 / 0.888 | 0.692 / 0.681 | 0.556 / 0.520 | 0.848 / 0.844 |
| Ovis2-5-9B | 0.831 / 0.822 | 0.896 / 0.895 | 0.724 / 0.694 | 0.657 / 0.596 | 0.864 / 0.860 |

alization from generic IQA to AIGI interior scenes.

Deep Learning-based NR-IQA: While offering improvements over traditional baselines, these models still achieve only moderate correlations on SA-BENCH. Q-Eval-Score leads in layout (0.265/0.266) and overall performance within this group (0.162/0.168). Q-Align-aesthetics excels in harmony (0.318/0.320), DeQA-Score in lighting (0.305/0.351), and Q-SiT in distortion (0.184/0.131). Despite these gains, their absolute correlations remain substantially lower than those of SFT-based VLMs, particularly for lighting and distortion.

Commercial MLLMs: Among closed-source commercial systems, gemini-2.5-pro demonstrates the strongest competitive performance, ranking first in multiple dimensions and overall score (0.414/0.393). Qwen-VL-Max is the next strongest overall (0.362/0.359). Notably, all commercial models struggle with lighting, often yielding near-zero or negative correlations, suggesting limitations in modeling photometric realism and shadow nuances in interior environments.

MLLMs (SFT-based): SFT substantially boosts spatial-aesthetics IQA. Our SA-IQA model, leveraging supervised fine-tuning, achieves state-of-the-art results across all dimensions. It delivers the best performance in layout (0.831/0.822), harmony (0.896/0.895), lighting (0.724/0.694), distortion (0.657/0.596), and overall (0.864/0.860). Compared to the strongest non-our baseline (e.g., Qwen3-VL-8B, overall 0.849/0.846), SA-IQA consistently demonstrates significant improvements, particularly in PLCC for layout and lighting, while maintaining competitiveness in distortion.

These results reveal three key insights: (1) traditional and generic IQA models are ineffective for the multi-dimensional complexities of interior AIGI; (2) general-purpose commercial MLLMs capture stylistic harmony but fall short in robustly assessing lighting and distortion; and (3) aligning MLLMs through supervised fine-tuning on SA-BENCH, combined with multi-dimensional reward evaluation, leads to substantial and consistent gains, establishing a new state of the art on SA-BENCH.

4.3. Ablation Studies

Prompt Style Analysis. We investigated four prompt styles for SA-IQA, ranging from concise (Type 1: single short sentence; Type 2: concise with special characters) to detailed (Type 3: multi-sentence natural language; Type 4: expert-aware with domain-specific terminology). Our findings indicate that prompt quality, particularly its detail and professional alignment, is crucial. **Expert-Aware Prompts** consistently achieve the best Overall correlation (0.864/0.860) and strongest Distortion score (0.657/0.596). While Detailed Prompts excel in Harmony (0.898/0.896), Concise+ Prompts offer marginal improvements in Lighting (0.729/0.711). Layout scores remain relatively stable across styles, with a slight advantage for Expert-Aware Prompts (0.831/0.822). This suggests that detailed, professional, and dimension-aware instructions significantly enhance PLCC/SRCC, whereas mere conciseness or special characters provide limited benefits.

Effect of model size. We investigate the impact of model size on SA-IQA performance by comparing Qwen3-VL (2B, 4B, 8B) and Ovis2.5 (2B, 9B), as summarized in Table 5. Scaling Qwen3-VL from 2B to 4B significantly improves Overall correlation (from 0.841/0.836 to 0.853/0.849), particularly boosting Lighting and Distortion scores. However, further scaling to 8B does not yield additional gains (0.849/0.846), suggesting a performance saturation without stronger alignment strategies. For our Ovis2.5 model, scaling to 9B, specifically enhanced with SA-IQA SFT, achieves the best Overall performance (0.864/0.860), demonstrating substantial improvements in Lighting (0.724/0.694) and Distortion (0.657/0.596). This ablation highlights that while moderate model scaling is beneficial, integrating a larger backbone with our SA-IQA SFT is crucial for achieving state-of-the-art results, especially for accurate photometric realism and deformation assessment.

4.4. Reinforcement Learning with GRPO

To demonstrate the efficacy of SA-IQA as a reward signal, we integrate it into the reinforcement learning frame-



Figure 5. **Qualitative Visualization of RL Improvement.** This figure presents generated background examples from the intermediate training results of our RL process

work to optimize a prompt expansion module for generative background-completion model. The optimization process involves two stages: (1) LoRA-based SFT on Qwen2.5-VL-7B, followed by (2) GRPO training initialized from the SFT checkpoint, utilizing SA-IQA as the core reward. We configured the GRPO with a group size of 8 and a batch size of 4.

Through this optimization, the average SA-IQA reward significantly increase from 0.70 to **0.86**, accompanied by a reduction in standard deviation from 0.12 to **0.06**. This quantitative improvement indicates both higher generated quality and enhanced stability.

Figure 5 visually substantiates these gains. Each row of the figure corresponds to a different training epoch, showcasing the progression of optimization. Within each row, three images are selected from a GRPO group of eight, specifically the 1st, 3rd, and 5th images when sorted by their SA-IQA reward in ascending order. The qualitative comparison clearly illustrates that RL training, guided by SA-IQA, consistently leads to more coherent structural layouts, realistic lighting, and reduced distortions in the generated backgrounds across different epochs.

4.5. Best-of-N Evaluation

To further validate SA-IQA’s utility as a generation quality controller, we apply a Best-of- N (BoN) filtering strategy. For each generation prompt, the model samples $N = 4$ candidate images. SA-IQA then scores and re-ranks these candidates to select the optimal output.

As illustrated in Figure 6, SA-IQA effectively sorts candidates based on their spatial aesthetic quality. This re-ranking significantly elevates the final generation quality,



Figure 6. **Best-of- N Re-ranking for Quality Filtering.** Each row showcases generated images for a given prompt, sorted from lowest (left) to highest (right) SA-IQA assessed quality. SA-IQA consistently identifies and prioritizes aesthetically superior outputs for interior scenes.

demonstrating strong alignment with human preferences. The visual progression from lower to higher quality within each row confirms SA-IQA’s reliability in identifying the most aesthetically coherent results.

5. Conclusion

In this work, we present the first comprehensive study on spatial-aesthetic Image Quality Assessment (IQA) for interior scenes. To this end, we introduce **SA-BENCH**, the first large-scale, multi-dimensional benchmark comprising 18k images with 50k annotations across four critical dimensions: **layout, harmony, lighting, and distortion**.

Furthermore, we propose **SA-IQA**, a novel, reward-ready evaluation framework that achieves state-of-the-art performance. SA-IQA’s predictions demonstrate significantly higher PLCC/SROCC correlations with human Mean Opinion Scores (MOS) than existing methods across all four dimensions and overall. We also validate SA-IQA’s practical utility as a reward signal. When integrated with GRPO, SA-IQA consistently improves the spatial-aesthetic quality of generated outputs, while Best-of- N selection using our metric further amplifies the output quality. We anticipate this work will inspire and facilitate future research in spatial aesthetics for AI-based interior design.

References

- [1] Shuai Bai, Keqin Chen, Xuejing Liu, Jialin Wang, Wenbin Ge, Sibao Song, Kai Dang, Peng Wang, Shijie Wang, Jun Tang, et al. Qwen2. 5-vl technical report. *arXiv preprint arXiv:2502.13923*, 2025. 3
- [2] Ralph Allan Bradley and Milton E Terry. Rank analysis of incomplete block designs. I. The method of paired comparisons. *Biometrika*, 39(3/4):324–345, 1952. 5
- [3] Zheng Chen, Xun Zhang, Wenbo Li, Renjing Pei, Fenglong Song, Xiongkuo Min, Xiaohong Liu, Xin Yuan, Yong Guo, and Yulun Zhang. Grounding-iqa: Multimodal language grounding model for image quality assessment. *arXiv preprint arXiv:2411.17237*, 2024. 3
- [4] Patrick Esser, Sumith Kulal, Andreas Blattmann, Rahim Entezari, Jonas Müller, Harry Saini, Yam Levi, Dominik Lorenz, Axel Sauer, Frederic Boesel, et al. Scaling rectified flow transformers for high-resolution image synthesis. In *Forty-first international conference on machine learning*, 2024. 2
- [5] Stephanie Fu, Netanel Tamir, Shobhita Sundaram, Lucy Chai, Richard Zhang, Tali Dekel, and Phillip Isola. Dreamsim: Learning new dimensions of human visual similarity using synthetic data. *arXiv preprint arXiv:2306.09344*, 2023. 3
- [6] Yuan Gong, Xionghui Wang, Jie Wu, Shiyin Wang, Yitong Wang, and Xinglong Wu. Onereward: Unified mask-guided image generation via multi-task human preference learning. *arXiv preprint arXiv:2508.21066*, 2025. 1
- [7] Shuai He, Yongchang Zhang, Rui Xie, Dongxiang Jiang, and Anlong Ming. Rethinking image aesthetics assessment: Models, datasets and benchmarks. In *IJCAI*, pages 942–948, 2022. 1
- [8] Xuan Ju, Xian Liu, Xintao Wang, Yuxuan Bian, Ying Shan, and Qiang Xu. Brushnet: A plug-and-play image inpainting model with decomposed dual-branch diffusion. In *European Conference on Computer Vision*, pages 150–168. Springer, 2024. 2, 3
- [9] Junjie Ke, Qifei Wang, Yilin Wang, Peyman Milanfar, and Feng Yang. Musiq: Multi-scale image quality transformer. In *Proceedings of the IEEE/CVF International Conference on Computer Vision (ICCV)*, pages 5148–5157, 2021. 6
- [10] Yuval Kirstain, Adam Polyak, Uriel Singer, Shahbuland Matiana, Joe Penna, and Omer Levy. Pick-a-pic: An open dataset of user preferences for text-to-image generation. *Advances in neural information processing systems*, 36:36652–36663, 2023. 1, 4
- [11] Black Forest Labs, Stephen Batifol, Andreas Blattmann, Frederic Boesel, Saksham Consul, Cyril Diagne, Tim Dockhorn, Jack English, Patrick Esser, Rocky Ge, et al. Flux.1 kontext: Flow matching for in-context image generation and editing in latent space. *arXiv preprint arXiv:2506.15742*, 2025. 2, 3
- [12] Sangwu Lee, Titus Ebbecke, Erwann Millon, Will Beddow, Le Zhuo, Iker García-Ferrero, Liam Esparraguera, Mihai Petrescu, Gian Saß, Gabriel Menezes, and Victor Perez. Flux.1 krea [dev], 2025. 2
- [13] Chunyi Li, Zicheng Zhang, Haoning Wu, Wei Sun, Xiongkuo Min, Xiaohong Liu, Guangtao Zhai, and Weisi Lin. Aigqa-3k: An open database for ai-generated image quality assessment. *IEEE Transactions on Circuits and Systems for Video Technology*, 34(8):6833–6846, 2023. 2, 4
- [14] Chunyi Li, Tengchuan Kou, Yixuan Gao, Yuqin Cao, Wei Sun, Zicheng Zhang, Yingjie Zhou, Zhichao Zhang, Weixia Zhang, Haoning Wu, et al. Aigqa-20k: A large database for ai-generated image quality assessment. In *Proceedings of the IEEE/CVF Conference on Computer Vision and Pattern Recognition*, pages 6327–6336, 2024. 1, 2
- [15] Weiqi Li, Xuanyu Zhang, Shijie Zhao, Yabin Zhang, Junlin Li, Li Zhang, and Jian Zhang. Q-insight: Understanding image quality via visual reinforcement learning. *arXiv preprint arXiv:2503.22679*, 2025. 3, 6
- [16] Yunhao Li, Sijing Wu, Wei Sun, Zhichao Zhang, Yucheng Zhu, Zicheng Zhang, Huiyu Duan, Xiongkuo Min, and Guangtao Zhai. Aghi-qa: A subjective-aligned dataset and metric for ai-generated human images. *arXiv preprint arXiv:2504.21308*, 2025. 1, 2
- [17] S. Lu and et al. Ovis2.5: A successor to ovis2 for native-resolution visual perception and multimodal reasoning. Technical report, Alibaba Group / AIDC-AI, 2025. Technical Report, arXiv:2508.11737. 5, 6
- [18] Dustin Podell, Zion English, Kyle Lacey, Andreas Blattmann, Tim Dockhorn, Jonas Müller, Joe Penna, and Robin Rombach. Sdxl: Improving latent diffusion models for high-resolution image synthesis, 2023. 2
- [19] Qwen Team. Qwen3-VL: Sharper Vision, Deeper Thought, Broader Action, 2025. A Technical Report on the Qwen3-VL Model Series. 6
- [20] Robin Rombach, Andreas Blattmann, Dominik Lorenz, Patrick Esser, and Björn Ommer. High-resolution image synthesis with latent diffusion models. In *Proceedings of the IEEE/CVF conference on computer vision and pattern recognition*, pages 10684–10695, 2022. 2, 3
- [21] Team Seedream, :, Yunpeng Chen, Yu Gao, Lixue Gong, Meng Guo, Qiushan Guo, Zhiyao Guo, Xiaoxia Hou, Weilin Huang, Yixuan Huang, Xiaowen Jian, Huafeng Kuang, Zhichao Lai, Fanshi Li, Liang Li, Xiaochen Lian, Chao Liao, Liyang Liu, Wei Liu, Yanzuo Lu, Zhengxiong Luo, Tongtong Ou, Guang Shi, Yichun Shi, Shiqi Sun, Yu Tian, Zhi Tian, Peng Wang, Rui Wang, Xun Wang, Ye Wang, Guofeng Wu, Jie Wu, Wenxu Wu, Yonghui Wu, Xin Xia, Xuefeng Xiao, Shuang Xu, Xin Yan, Ceyuan Yang, Jianchao Yang, Zhonghua Zhai, Chenlin Zhang, Heng Zhang, Qi Zhang, Xinyu Zhang, Yuwei Zhang, Shijia Zhao, Wenliang Zhao, and Wenjia Zhu. Seedream 4.0: Toward next-generation multimodal image generation, 2025. 2
- [22] Shaolin Su, Qingsen Yan, Yu Zhu, Cheng Zhang, Xin Ge, Jinqiu Sun, and Yanning Zhang. Blindly assess image quality in the wild guided by a self-adaptive hyper network. In *Proceedings of the IEEE/CVF conference on computer vision and pattern recognition*, pages 3667–3676, 2020. 6
- [23] Jianyi Wang, Kelvin CK Chan, and Chen Change Loy. Exploring clip for assessing the look and feel of images. In *Proceedings of the AAAI conference on artificial intelligence*, pages 2555–2563, 2023. 1, 6

- [24] Jiarui Wang, Huiyu Duan, Jing Liu, Shi Chen, Xiongkuo Min, and Guangtao Zhai. Aigciqa2023: A large-scale image quality assessment database for ai generated images: from the perspectives of quality, authenticity and correspondence. In *CAAI International Conference on Artificial Intelligence*, pages 46–57. Springer, 2023. 2
- [25] Weiyun Wang, Zhangwei Gao, Lixin Gu, Hengjun Pu, Long Cui, Xingguang Wei, Zhaoyang Liu, Linglin Jing, Shenglong Ye, Jie Shao, et al. Internv13. 5: Advancing open-source multimodal models in versatility, reasoning, and efficiency. *arXiv preprint arXiv:2508.18265*, 2025. 6
- [26] Zijie J Wang, Evan Montoya, David Munechika, Haoyang Yang, Benjamin Hoover, and Duen Horng Chau. Diffusiondb: A large-scale prompt gallery dataset for text-to-image generative models. In *Proceedings of the 61st Annual Meeting of the Association for Computational Linguistics (Volume 1: Long Papers)*, pages 893–911, 2023. 4
- [27] Haoning Wu, Zicheng Zhang, Weixia Zhang, Chaofeng Chen, Liang Liao, Chunyi Li, Yixuan Gao, Annan Wang, Erli Zhang, Wenxiu Sun, et al. Q-align: Teaching Imms for visual scoring via discrete text-defined levels. *arXiv preprint arXiv:2312.17090*, 2023. 1, 2, 5, 6
- [28] Xiaoshi Wu, Yiming Hao, Keqiang Sun, Yixiong Chen, Feng Zhu, Rui Zhao, and Hongsheng Li. Human preference score v2: A solid benchmark for evaluating human preferences of text-to-image synthesis. *arXiv preprint arXiv:2306.09341*, 2023. 2
- [29] Xiaoshi Wu, Keqiang Sun, Feng Zhu, Rui Zhao, and Hongsheng Li. Human preference score: Better aligning text-to-image models with human preference. In *Proceedings of the IEEE/CVF International Conference on Computer Vision*, pages 2096–2105, 2023. 4
- [30] Xiaoshi Wu, Keqiang Sun, Feng Zhu, Rui Zhao, and Hongsheng Li. Better aligning text-to-image models with human preference. *arXiv preprint arXiv:2303.14420*, 1(3), 2023. 1
- [31] Jiazheng Xu, Xiao Liu, Yuchen Wu, Yuxuan Tong, Qinkai Li, Ming Ding, Jie Tang, and Yuxiao Dong. Imagereward: Learning and evaluating human preferences for text-to-image generation. *Advances in Neural Information Processing Systems*, 36:15903–15935, 2023. 2
- [32] J. Xu, X. Liu, Y. Wu, et al. ImageReward: Learning and Evaluating Human Preferences for Text-to-Image Generation. In *NeurIPS*, 2023. 4
- [33] Sidi Yang, Tianhe Wu, Shuwei Shi, Shanshan Lao, Yuan Gong, Mingdeng Cao, Jiahao Wang, and Yuj Yang. Maniqa: Multi-dimension attention network for no-reference image quality assessment. In *Proceedings of the IEEE/CVF Conference on Computer Vision and Pattern Recognition (CVPR)*, pages 1191–1200, 2022. 6
- [34] Xiaohan Yang, Fan Li, and Hantao Liu. A survey of dnn methods for blind image quality assessment. *IEEE Access*, 7:123788–123806, 2019. 1
- [35] Jiabo Ye, Haiyang Xu, Haowei Liu, Anwen Hu, Ming Yan, Qi Qian, Ji Zhang, Fei Huang, and Jingren Zhou. mplug-owl3: Towards long image-sequence understanding in multimodal large language models. Technical report, X-PLUG Lab, 2024. arXiv:2408.04840. ICLR 2025 poster version exists. 6
- [36] Ran Yi, Haoyuan Tian, Zhihao Gu, Yu-Kun Lai, and Paul L Rosin. Towards artistic image aesthetics assessment: a large-scale dataset and a new method. In *Proceedings of the IEEE/CVF Conference on Computer Vision and Pattern Recognition*, pages 22388–22397, 2023. 1
- [37] Zhiyuan You, Xin Cai, Jinjin Gu, Tianfan Xue, and Chao Dong. Teaching large language models to regress accurate image quality scores using score distribution. In *IEEE Conference on Computer Vision and Pattern Recognition (CVPR) 2025*, 2025. 6
- [38] Zihao Yu, Fengbin Guan, Yiting Lu, Xin Li, and Zhibo Chen. Sf-iqa: Quality and similarity integration for ai generated image quality assessment. In *Proceedings of the IEEE/CVF Conference on Computer Vision and Pattern Recognition*, pages 6692–6701, 2024. 1
- [39] Team GLM: Aohan Zeng, Bin Xu, Yuxiao Dong, and Jie Tang. Chatglm: A family of large language models from glm-130b to glm-4 all tools, 2024. 6
- [40] Weixia Zhang, Kede Ma, Jia Yan, Dexiang Deng, and Zhou Wang. Blind image quality assessment using a deep bilinear convolutional neural network. *IEEE Transactions on Circuits and Systems for Video Technology*, 30(1):36–47, 2018. 6
- [41] Yuxuan Zhang, Yirui Yuan, Yiren Song, Haofan Wang, and Jiaming Liu. Easycontrol: Adding efficient and flexible control for diffusion transformer. *arXiv preprint arXiv:2503.07027*, 2025. 2, 3
- [42] Zicheng Zhang, Chunyi Li, Wei Sun, Xiaohong Liu, Xiongkuo Min, and Guangtao Zhai. A perceptual quality assessment exploration for aigc images. In *2023 IEEE International Conference on Multimedia and Expo Workshops (ICMEW)*, pages 440–445. IEEE, 2023. 4
- [43] Zicheng Zhang, Tengchuan Kou, Shushi Wang, Chunyi Li, Wei Sun, Wei Wang, Xiaoyu Li, Zongyu Wang, Xuezhi Cao, Xiongkuo Min, et al. Q-eval-100k: Evaluating visual quality and alignment level for text-to-vision content. In *Proceedings of the Computer Vision and Pattern Recognition Conference*, pages 10621–10631, 2025. 6
- [44] Zicheng Zhang, Haoning Wu, Ziheng Jia, Weisi Lin, and Guangtao Zhai. Teaching Imms for image quality scoring and interpreting. *arXiv preprint arXiv:2503.09197*, 2025. 6
- [45] Peng Zheng, Dehong Gao, Deng-Ping Fan, Li Liu, Jorma Laaksonen, Wanli Ouyang, and Nicu Sebe. Bilateral reference for high-resolution dichotomous image segmentation. *arXiv preprint arXiv:2401.03407*, 2024. 3
- [46] Hanwei Zhu, Haoning Wu, Yixuan Li, Zicheng Zhang, Baoliang Chen, Lingyu Zhu, Yuming Fang, Guangtao Zhai, Weisi Lin, and Shiqi Wang. Adaptive image quality assessment via teaching large multimodal model to compare. In *arXiv preprint arXiv:2405.19298*, 2024. 6

SA-IQA: Redefining Image Quality Assessment for Spatial Aesthetics with Multi-Dimensional Rewards

Supplementary Material

A. Overview

This Supplementary Material provides additional details regarding our work on SA-IQA. It is structured as follows: Section B elaborates on prompt design strategies. Section C details the SA-BENCH dataset, including annotation results and data distributions. Section D covers our algorithmic methodology, including data preprocessing, inference scoring, and reinforcement learning with GRPO. Section E presents further experimental details on multi-dimensional fusion and training strategies. Finally, Sections F and G provide additional SA-IQA inference examples and discuss limitations and societal impact, respectively.

B. Prompt Design

B.1. SA-IQA Prompts

The SA-IQA framework utilizes four distinct prompt types, varying from concise to detailed, which were designed for ablation studies. These types include: (1) single short sentences, (2) concise prompts enhanced with special characters, (3) multi-sentence natural language descriptions, and (4) expert-aware prompts incorporating domain-specific terminology. The specific prompts are listed below:

Type 1 (Concise)

- Query: <image>Please evaluate the spatial aesthetic {dimension} quality level of this image. Response: The spatial aesthetic {dimension} quality level of this image is {rating_word}.

Type 2 (Concise with Special Characters)

- Query: <image><{dimension}>Please evaluate the spatial aesthetic {dimension} quality level of this image. Response: The spatial aesthetic {dimension} quality level of this image is {rating_word}.

Type 3 (Detailed, General Description)

- Query: <image><layout>Please evaluate the spatial aesthetic layout quality level of this image. The layout dimension describes the spatial distribution and positional relationships of major elements within a composition. Assess how the layout contributes to the overall organization, structure, and balance of the image. Response: The spatial

aesthetic layout quality level of this image is {rating_word}.

- Query: <image><harmony>Please evaluate the spatial aesthetic harmony quality level of this image. The harmony dimension emphasizes stylistic consistency, color matching, and overall visual coordination. Consider how well the elements come together to create a unified and pleasing appearance. Response: The spatial aesthetic harmony quality level of this image is {rating_word}.
- Query: <image><lighting>Please evaluate the spatial aesthetic lighting quality level of this image. The lighting dimension focuses on the interaction between light and shadow, including the quality of lighting effects and the sense of three-dimensionality. Assess how lighting enhances or affects the depth and overall atmosphere of an image. Response: The spatial aesthetic lighting quality level of this image is {rating_word}.
- Query: <image><distortion>Please evaluate the spatial aesthetic distortion quality level of this image. The distortion dimension describes the degree of distortion in shapes or the fidelity of background details. Assess how the distortion impacts the perceived realism and visual quality of the image. Response: The spatial aesthetic distortion quality level of this image is {rating_word}.

Type 4 (Detailed, Expert-Aware Description)

- Query: <image><layout>Please evaluate the spatial aesthetic layout quality level of this image. The layout dimension describes the spatial distribution, positional relationships, and quantity of major elements within the space. Consider how the layout supports the overall visual order, maintains balance, and

enhances the functional aesthetics of the image. **Response:** The spatial aesthetic layout quality level of this image is {rating_word}.

- **Query:** <image><harmony>Please evaluate the spatial aesthetic harmony quality level of this image. The harmony dimension focuses on stylistic consistency, color coordination, and overall visual cohesion. Examine how well the combination of elements creates a balanced and visually pleasant composition, avoiding clashes or imbalances in style and color. **Response:** The spatial aesthetic harmony quality level of this image is {rating_word}.
- **Query:** <image><lighting>Please evaluate the spatial aesthetic lighting quality level of this image. The lighting dimension examines the quality of light effects, shadow interactions, and the realism of light sources. Assess how well lighting contributes to the overall depth, mood, and authenticity of the image, emphasizing both natural and artificial lighting scenarios. **Response:** The spatial aesthetic lighting quality level of this image is {rating_word}.
- **Query:** <image><distortion>Please evaluate the spatial aesthetic distortion quality level of this image. The distortion dimension assesses whether soft furnishings (e.g., cabinets, carpets) or fixed structures (e.g., floors, walls) appear deformed or misaligned. Additionally, evaluate the realism and material accuracy of textures, and judge whether any distortion negatively impacts the overall aesthetic quality of the image. **Response:** The spatial aesthetic distortion quality level of this image is {rating_word}.

B.2. Commercial Model Prompts

To benchmark commercial closed-source models on SA-BENCH, we adapted the expert-aware prompts (Type 4) from SA-IQA. The refined prompts used for querying these models are as follows:

- **Prompt 1 (Layout):** You are an interior

spatial aesthetics evaluation assistant. The input is an image of an interior space. Please evaluate the spatial aesthetic layout quality level of this image. The layout dimension describes the spatial distribution, positional relationships, and quantity of major elements within the space. Consider how the layout supports the overall visual order, maintains balance, and enhances the functional aesthetics of the image. Output only one score from [1,2,3,4,5], where a higher score indicates higher quality. Return in the format {"score": score}.

- **Prompt 2 (Harmony):** You are an interior spatial aesthetics evaluation assistant. The input is an image of an interior space. Please evaluate the spatial aesthetic harmony quality level of this image. The harmony dimension focuses on stylistic consistency, color coordination, and overall visual cohesion. Examine how well the combination of elements creates a balanced and visually pleasant composition, avoiding clashes or imbalances in style and color. Output only one score from [1,2,3,4,5], where a higher score indicates higher quality. Return in the format {"score": score}.
- **Prompt 3 (Lighting):** You are an interior spatial aesthetics evaluation assistant. The input is an image of an interior space. Please evaluate the spatial aesthetic lighting quality level of this image. The lighting dimension examines the quality of light effects, shadow interactions, and the realism of light sources. Assess how well lighting contributes to the overall depth, mood, and authenticity of the image, emphasizing both natural and artificial lighting scenarios. Output only one score from [1,2,3,4,5], where a higher score indicates higher quality. Return in the format {"score": score}.
- **Prompt 4 (Distortion):** You are an interior spatial aesthetics evaluation assistant. The input is an image of

Table 6. Definitions and Specific Criteria for Spatial Aesthetic Dimensions.

| Dimension | Description and Specific Criteria |
|-------------------|--|
| Layout | <p>Definition: Spatial arrangement of key elements, their relative positions, and object counts. Typical problems include excessive emptiness, clutter, and poor placement.</p> <p>Specific Criteria: All objects exhibit logical positional relationships, avoiding <i>Floating Objects</i>, <i>Unconventional Placement</i>. Objects should be placed according to design function and common design practices. The quantity of items should be appropriate, avoiding <i>Excessive Clutter</i> or <i>Excessive Emptiness</i>. For close-up shots where main items like chairs or cabinets occupy a large proportion, fewer auxiliary items are acceptable but not excessive.</p> |
| Harmony | <p>Definition: Stylistic coherence, color compatibility, and overall visual consistency. Typical problems include color clashes, mismatched design styles, and generally unattractive appearance.</p> <p>Specific Criteria: The overall style is unified, avoiding <i>Inconsistent Style</i> or obvious incongruity. Color schemes are coordinated and consistent with the design style, avoiding <i>Discordant Colors</i>. The image adheres to popular aesthetic trends, avoiding <i>Poor Aesthetics</i>, outdated, or unattractive styles.</p> |
| Lighting | <p>Definition: Quality of illumination, shadow behavior, and realism of light sources. Typical problems include unnatural lighting, incorrect or inconsistent shadows, and implausible light sources.</p> <p>Specific Criteria: Prevents <i>Over-Bright/Unrealistic Light</i>, such as overexposure due to overly strong or unrealistic light. Ensures <i>Unrealistic Shadows</i> are avoided, preventing uniformly bright or dark scenes, and ensuring shadow directions align logically with light sources. Light sources are logically and realistically placed, thereby avoiding an <i>Implausible Light Source</i>.</p> |
| Distortion | <p>Definition: Geometric or semantic deformation of furnishings/fixtures and the realism of materials. Typical problems include warped or distorted backgrounds, shape deformation, and unconvincing materials.</p> <p>Specific Criteria: Soft furnishings (various objects) and hard fixtures (e.g., ceilings, walls, floors) are not subjected to <i>Soft Furnishing Deformation</i> or <i>Hard Fixture Deformation</i>, meaning they are not deformed, warped, or misaligned. Material effects are realistic, with appropriate textures and proportions, avoiding <i>Unrealistic Materials</i>, deformation, stretching, or blurriness.</p> |

an interior space. Please evaluate the spatial aesthetic distortion quality level of this image. The distortion dimension assesses whether soft furnishings (e.g., cabinets, carpets) or fixed structures (e.g., floors, walls) appear deformed or misaligned. Additionally, evaluate the realism and material accuracy of textures, and judge whether any distortion negatively impacts the overall aesthetic quality of the image. Output only one score from [1,2,3,4,5], where a higher score indicates higher quality. Return in the format {"score": score}.

C. Dataset Details

C.1. Annotation Results for Four Dimensions

We define four spatial aesthetic dimensions for image quality assessment: Layout, Harmony, Lighting, and Distortion. Their definitions and specific criteria, guiding our annota-

tion process, are summarized in Table 6.

Rating Scale. Annotations utilize a 5-point Likert scale, where 1 (significant major issue) corresponds to *bad*, 2 (noticeable minor issue) to *poor*, 3 (subtle minor issue) to *fair*, 4 (slight flaw) to *good*, and 5 (no issue) to *excellent*.

Visual Annotation Examples. Visualizations of our annotation results are presented in Figures 7 to 11. Specifically, Figures 7, 8, 10, and 9 showcase annotation samples for Layout, Harmony, Lighting, and Distortion, respectively, where image quality gradually improves from left to right within each row’s problem type. Figure 11 provides examples of images that received an “excellent” quality rating across all four dimensions.

C.2. Data Distribution

The data distribution for the training and testing sets across all four dimensions of SA-BENCH is visualized in Figure 12. It can be observed that the distributions for both the training and testing sets are consistent for each dimension.



Figure 7. **Layout Dimension Annotation Example.** Each row illustrates a specific problem type within the Layout dimension, with image quality incrementally improving from left to right.

D. Methodology Details

D.1. Data Preprocessing

After data annotation, two key steps were performed for quality control:

Rater Reliability We evaluate annotator consistency by computing the Spearman’s Rank Correlation Coefficient (SRCC) between each individual annotator’s scores and the aggregated Mean Opinion Score (MOS). Annotators whose SRCC falls below 0.6 are flagged for further review to ensure data quality. The SRCC is calculated as:

$$\text{SRCC} = 1 - \frac{6 \sum d_i^2}{n(n^2 - 1)} \quad (4)$$

where d_i is the difference between the ranks of corresponding observations, and n is the number of observations.

Outlier Mitigation We standardize ratings using the z-score to identify and mitigate outliers. Ratings with an absolute z-score > 2 are replaced by the mean score for that image, and the MOS is recomputed. The z-score is calculated as:

$$z = \frac{x - \mu}{\sigma} \quad (5)$$

where x is an individual rating, μ is the mean of all ratings for a given image, and σ is the standard deviation of all



ratings for that image.

D.2. Inference Scoring

To bridge the gap between the categorical text ratings generated by the MLLM and a continuous MOS, we employ a probabilistic conversion method. This process involves two main steps:

Softmax Normalization. We first extract the top-5 probabilities corresponding to the five predefined rating words (e.g., excellent, good, fair, poor, bad) from the MLLM’s final quality word token. These raw probabilities are then normalized using the softmax function to ensure they sum to 1. The softmax function is defined as:

$$P_i = \frac{e^{\text{logits}_i}}{\sum_{j=1}^K e^{\text{logits}_j}} \quad (6)$$

where P_i is the normalized probability for rating word i , logits_i is the logit for rating word i directly from the MLLM, and $K = 5$ is the total number of rating words.

Weighted Sum for Final Score. After obtaining the normalized probabilities, we compute the expected value by mapping these probabilities to a 1-5 scale (e.g., excellent \rightarrow 5, good \rightarrow 4, fair \rightarrow 3, poor \rightarrow 2,

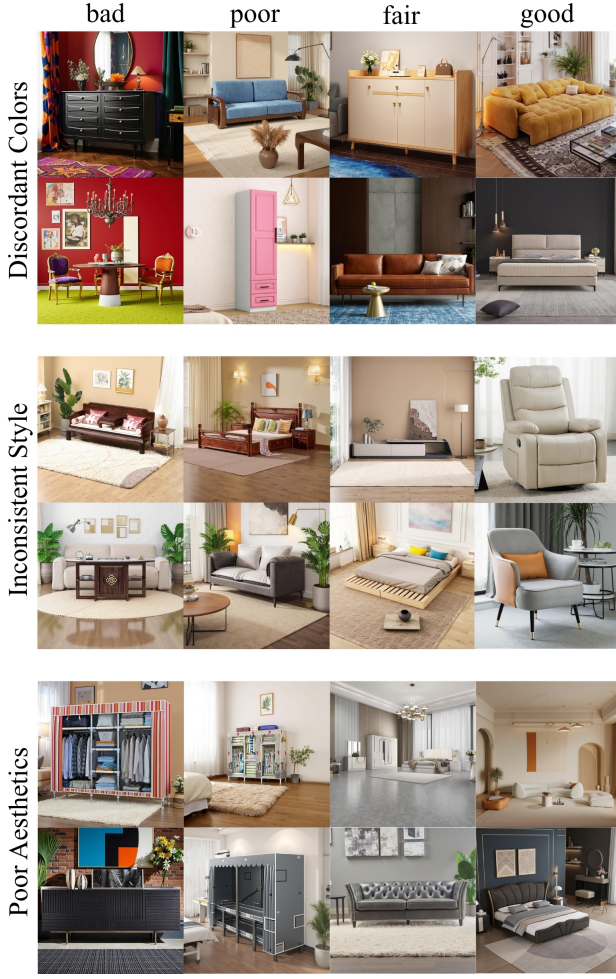


Figure 8. **Harmony Dimension Annotation Example.** Similar to Harmony, each row depicts a problem type, showing improving quality from left to right.

bad \rightarrow 1). This yields the final continuous score within the range [1, 5]. The weighted sum formula is:

$$\text{Score} = \sum_{i=1}^K (P_i \times \text{rating_value}_i) \quad (7)$$

where P_i is the normalized probability for rating word i , and rating_value_i is its corresponding numerical value on the 1-5 scale.

D.3. Reinforcement Learning with GRPO

We integrate SA-IQA into a reinforcement learning framework to optimize a prompt expansion module for a generative background-completion model. This optimization involves LoRA-based SFT on Qwen2.5-VL-7B, followed by GRPO training (with a group size of 8 and batch size of 4) initialized from the SFT checkpoint, where SA-IQA serves as the core reward signal.



Figure 9. **Distortion Dimension Annotation Example.** Each row demonstrates a type of Distortion problem, with image quality increasing from left to right.

The calculation formula for GRPO is presented below:

$$\begin{aligned} \mathcal{J}_{GRPO}(\theta) = & \mathbb{E} \left[q \sim P(Q), \{o_i\}_{i=1}^G \sim \pi_{\theta_{old}}(O|q) \right] \\ & \frac{1}{G} \sum_{i=1}^G \frac{1}{|o_i|} \sum_{t=1}^{|o_i|} \left\{ \min \left[\frac{\pi_{\theta}(o_{i,t}|q, o_{i,<t})}{\pi_{\theta_{old}}(o_{i,t}|q, o_{i,<t})} \hat{A}_{i,t}, \right. \right. \\ & \left. \left. \text{clip} \left(\frac{\pi_{\theta}(o_{i,t}|q, o_{i,<t})}{\pi_{\theta_{old}}(o_{i,t}|q, o_{i,<t})}, 1 - \epsilon, 1 + \epsilon \right) \hat{A}_{i,t} \right] \right. \\ & \left. - \beta \mathbb{D}_{KL} [\pi_{\theta} || \pi_{ref}] \right\} \quad (8) \end{aligned}$$

where π_{θ} and $\pi_{\theta_{old}}$ denote the current policy and the old sampling policy, respectively; π_{ref} is the reference policy used for KL divergence regularization with coefficient β . The expectation is taken over a group of G outputs $\{o_i\}_{i=1}^G$ sampled for a query q . $\hat{A}_{i,t}$ represents the advantage value for the t -th token of the i -th output, which is computed



Figure 10. **Lighting Dimension Annotation Example.** Image quality for various Lighting issues progressively improves from left to right in each row.



Figure 11. **Excellent Quality Examples Across All Four Dimensions.** Illustrative images receiving “excellent” quality ratings across all four spatial aesthetic dimensions (Layout, Harmony, Lighting, and Distortion).

based on the rewards provided by SA-IQA relative to the group average. ϵ is the clipping parameter used to constrain the policy update.

E. Experimental Details

E.1. Multi-Dimensional Fusion Comparison

Our proposed SA-IQA framework, particularly its multi-dimensional fusion strategy, serves as a crucial reward mechanism for optimizing AI-generated content (AIGC)

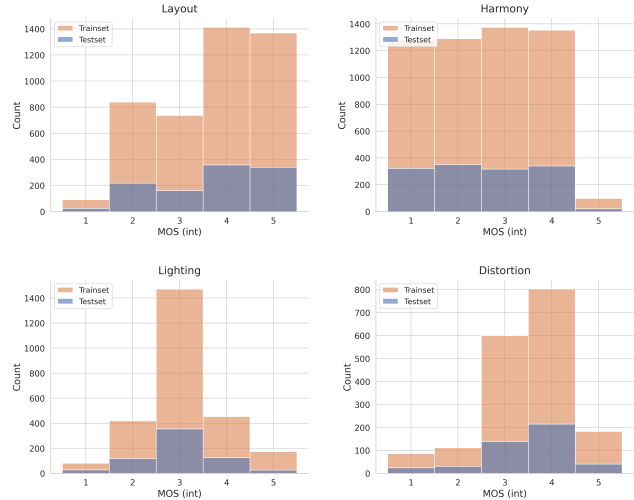


Figure 12. **Distribution of SA-BENCH Across Spatial Aesthetic Dimensions.** This figure shows the Mean Opinion Score (MOS) distributions for SA-BENCH’s training and testing sets across four spatial aesthetic dimensions: Layout, Harmony, Lighting, and Distortion. Scores are quantized (1-5) for clarity.

Table 7. Multi-Dimensional Fusion Comparison on Reward-Benchmark for Ranking Accuracy. **Bold** indicates the best performance.

| Eval Dimension | Threshold | Rank Accuracy |
|------------------------|-----------|---------------|
| Layout | 0.15 | 0.457 |
| Harmony | 0.27 | 0.541 |
| Lighting | 0.22 | 0.449 |
| Distortion | 0.22 | 0.440 |
| Equal Weighting (4D) | 0.37 | 0.503 |
| Optimal Weighting (4D) | 0.32 | 0.567 |

pipelines via reinforcement learning, specifically with GRPO. To validate the effectiveness of our fusion approach, we evaluate its ranking accuracy on a custom reward-benchmark designed to assess overall aesthetic quality across the four dimensions.

We investigate three distinct fusion settings:

- Individual Single-Dimension Models:** Each of the four dimensions (Layout, Harmony, Lighting, Distortion) is evaluated independently.
- Equal-Weighted Fusion (1:1:1:1):** The scores from the four dimensions are combined with equal weighting.
- Optimal Weighting (via *bt-loss*):** Fusion is performed using adaptively learned weights, optimized through a *bt-loss* mechanism.

The “Threshold” column in Table 7 represents a dynamically optimized threshold for each ranking method. In our pairwise comparison setup, where two images are evalu-

Table 8. Impact of Training Strategies (PLCC/SRCC) on SA-IQA Performance.

| Training Method | Layout | Harmony | Lighting | Distortion | Overall |
|------------------|---------------|---------------|---------------|---------------|---------------|
| LoRA Fine-tuning | 0.374 / 0.371 | 0.707 / 0.707 | 0.549 / 0.531 | 0.183 / 0.237 | 0.642 / 0.617 |
| Full Fine-tuning | 0.831 / 0.822 | 0.896 / 0.895 | 0.724 / 0.694 | 0.657 / 0.596 | 0.864 / 0.860 |

ated, results can be ‘win’, ‘lose’, or ‘tie’. This threshold (ranging from 1 to 5) defines that if the absolute difference between the continuous scores of two images falls below it, the comparison is registered as a ‘tie’.

Table 7 confirms the efficacy of multi-dimensional fusion. Optimal Weighting (via *bt-loss*) significantly outperforms individual single-dimension models and Equal Weighting in ranking accuracy. Harmony shows stronger individual performance, aligning with its higher weight in optimal fusion. Equal Weighting’s underperformance relative to the best individual dimension underscores the critical role of adaptive weighting, as it is unduly influenced by less performant dimensions.

E.2. Training Strategy Impact

We investigate the impact of different training strategies on SA-IQA’s performance, specifically comparing LoRA (Low-Rank Adaptation) fine-tuning against full model fine-tuning. Both strategies are applied to the SA-IQA algorithm, fine-tuned on the Ovis2-5-9B model. For LoRA training, the following specific parameters were employed: `lora.rank 32`, `lora.alpha 64`, `target_modules all-linear`, `freeze_llm false`, `freeze_vit true`, and `freeze_aligner true`. All other training parameters were kept consistent with those used for full fine-tuning. The comparative results, presented in Table 8, clearly demonstrate that full fine-tuning achieves superior performance compared to LoRA fine-tuning across all evaluated metrics.

F. SA-IQA Inference Case Studies

Figure 13 presents illustrative inference results of SA-IQA across diverse interior scene images. For each displayed image, the columns, from left to right, detail the predicted scores for the Layout, Harmony, Lighting, and Distortion dimensions, culminating in an aggregated Total Score. Notably, **bolded scores** signify dimensions where SA-IQA identifies significant quality deficiencies, providing a clear visual cue for specific aesthetic issues.

G. Limitations and Social Impact

Limitations. Our SA-IQA, while effective, has limitations. Computational constraints prevented exploring larger







| | Layout | Harmony | Lighting | Distortion | Total Score |
|---|---------------|---------------|---------------|---------------|-------------|
|  | 2.2582 | 3.3039 | 3.1975 | 4.1754 | 2.7768 |
|  | 4.3529 | 1.1414 | 3.9302 | 4.1301 | 2.0933 |
|  | 4.9134 | 2.6721 | 2.3005 | 3.9304 | 2.9591 |
|  | 4.0896 | 2.0211 | 3.7512 | 1.0131 | 2.0407 |
|  | 4.7495 | 4.1729 | 4.842 | 4.666 | 4.645 |
|  | 4.9699 | 4.0815 | 4.6506 | 4.9232 | 4.6362 |

Figure 13. **SA-IQA Inference Examples.** This figure demonstrates SA-IQA’s multi-dimensional scoring capabilities for interior images. Columns sequentially display scores for Layout, Harmony, Lighting, Distortion, and the overall Total Score. **Bolded** numerical values within a dimension indicate the presence of identified quality issues.

model scales (e.g., 32B or 72B parameters) and exhaustive GRPO hyper-parameter optimization, suggesting un-reached performance under ideal conditions. Its applicability to tasks needing deeper semantic reasoning or complex language understanding is also limited, as fine-tuning focused primarily on visual perception.

Social Impact. SA-IQA is poised to deliver significant positive societal impact by elevating the quality of AI-generated images (AIGI) and spatial design. It will empower designers to create more aesthetically pleasing and functional spaces, foster greater accessibility of high-quality visual content across various applications, and drive innovation in AI-driven design, ultimately enriching user experiences in both digital and physical realms.